ELSEVIER

International Journal of Mass Spectrometry 219 (2002) 315–324

International Journal of Mass Spectrometry

www.elsevier.com/locate/ijms

Some properties of charged particle trajectories in quadrupole mass spectrometers Part I. General theory

Ernst P. Sheretov

Department of Physics, Ryazan State Radio Technical University, Gagarin Street 59/1, 391000 Ryazan, Russia

Received 28 January 2002; accepted 29 May 2002

Abstract

A general theory of extreme characteristic solutions of the Hill equation is developed. The theory yields reliable expressions for calculation of amplitudes of charged particle oscillations within quadrupole mass spectrometers. It is demonstrated that trajectories of ions, operating points of which lie on quasi-stability lines (lines of modulation resonances), have remarkable features. Such ions have substantially smaller amplitudes than do those ions having operating points which do not lie on quasi-stability lines. The theory is quite general and can be applied for any rf waveform. A particular case of rectangular rf voltage is illustrated by equations for amplitude-phase characteristics (APC), applicable for ions with operating points lying on the quasi-stability line $\beta = 0$. It is demonstrated that APC of the first kind exhibits a flat region with relative amplitude of ion oscillation equal to 1. (Int J Mass Spectrom 219 (2002) 315–324)

Keywords: Mass spectrometry; Hill equation; Ion trap; Ion trap mass spectrometry

1. Introduction

The current state of quadrupole mass spectrometry (QMS) is characterized by a growing interest of mass spectrometrists towards injection of externally-generated ions into a quadrupole ion trap. To achieve this aim, one needs a reliable theory that determines amplitudes of ions injected into an rf field of a three-dimensional ion trap driven by a trapping rf voltage of arbitrary waveform. The theory of extreme characteristic solutions of the Hill equation, sequentially developed in our laboratory [1,2], yields simple analytical expressions for the amplitude of ion oscillation in quadrupole mass spectrometers [3] for an arbitrary set of initial conditions of ion motion and arbitrary rf waveforms. The use of this method, for instance, allowed us to optimize rf voltage waveform [4] and to achieve a new prospective waveform that we called the EC-signal.

When we checked the accuracy of expressions obtained by the method of extreme characteristic solutions, we found that the calculation error may reach 15–20% for some operating points in the stability diagram. Such an error occurred within a narrow range of stability parameters (for example, a and q values in the Mathieu equation) and could not be accounted for by the relatively small mean error. However, the development of ion trapping theory urged us to find

E-mail: sheretov@eac.ryazan.su

1387-3806/02/$ – see front matter
PII S1387-3806(02)00738-8

an appropiate explanation for this effect. As a result, a more general theory of extreme characteristic solutions was developed and its basic principles are explained in this paper.

2. General theory of extreme characteristic solutions of the Hill equation

Let us consider the Hill equation in the following form:

$$\ddot{y}(t) + \Phi(t)y(t) = 0 \tag{1}$$

where $\Phi(t)$ is a periodic function of period T_0. Basically, $\Phi(t)$ may have period of iT_0, where i is an integer (not equal to zero).

The general solutions of Eq. (1) are given by:

$$\begin{aligned} y(t) &= Ay_1(t) + By_2(t), \\ \dot{y}(t) &= A\dot{y}_1(t) + B\dot{y}_2(t) \end{aligned} \tag{2}$$

where $y_1(t)$ and $y_2(t)$ are two particular independent solutions of Eq. (1).

The following system is valid for $y_1(t)$ and $y_2(t)$:

$$\begin{vmatrix} y_1(t+T_0) \\ y_2(t+T_0) \end{vmatrix} = \begin{vmatrix} \alpha_1\alpha_2 \\ \beta_1\beta_2 \end{vmatrix} \times \begin{vmatrix} y_1(t) \\ y_2(t) \end{vmatrix} \tag{3}$$

where α_1, α_2, β_1 and β_2 are elements of the transformation matrix of partial solutions of Eq. (1).

Now, using Eqs. (2) and (3) we can obtain the following system for the general solution of Eq. (1):

$$\begin{aligned} y(t+T_0) &= \psi_3(t)y(t) + \psi_4(t)\dot{y}(t), \\ \dot{y}(t+T_0) &= \psi_1(t)y(t) + \psi_2(t)\dot{y}(t) \end{aligned} \tag{4}$$

For the $\psi_j(t)$ functions we have:

$$\begin{aligned} \psi_1(t)\gamma_0 &= \alpha_2\dot{y}_2^2(t) - \beta_1\dot{y}_1^2(t) + (\alpha_1 - \beta_2)\dot{y}_1(t)\dot{y}_2(t), \\ \psi_2(t)\gamma_0 &= \beta_1\dot{y}_1(t)y_1(t) - \alpha_2\dot{y}_2(t)y_2(t) \\ &\quad +\beta_2\dot{y}_2(t)y_1(t) - \alpha_1\dot{y}_1(t)y_2(t), \\ \psi_3(t)\gamma_0 &= \alpha_2\dot{y}_2(t)y_2(t) - \beta_1\dot{y}_1(t)y_1(t) \\ &\quad +\alpha_1\dot{y}_2(t)y_1(t) - \beta_2\dot{y}_1(t)y_2(t), \\ \psi_4(t)\gamma_0 &= \beta_1\dot{y}_1^2(t) - \alpha_2 y_2^2(t) + (\alpha_1 - \beta_2)y_2(t)y_1(t) \end{aligned} \tag{5}$$

Using Eq. (3) we can show that all the $\psi_j(t)$ functions are periodic functions of period T_0 and the following expressions are valid for them:

$$\begin{aligned} &\psi_2(t)\psi_3(t) - \psi_1(t)\psi_4(t) = 1, \\ &\psi_2(t) + \psi_3(t) = 2\beta_0 \end{aligned}$$

where β_0 is the stability parameter varying from -1 to $+1$ within a stable region.

It can be seen from Eq. (4) that $\psi_j(t)$ are elements of the transformation matrix of the general solution of the Hill equation.

It follows from Eq. (4) that:

$$\begin{aligned} y(t-T_0) &= \psi_2(t)y(t) - \psi_4(t)\dot{y}(t), \\ \dot{y}(t-T_0) &= -\psi_1(t)y(t) + \psi_3(t)\dot{y}(t) \end{aligned} \tag{6}$$

Now, using Eqs. (5) and (6) we can prove the validity of known recurrent formulas for general solutions of the Hill equation:

$$\begin{aligned} y(t+T_0) + y(t-T_0) &= 2\beta_0 y(t), \\ \dot{y}(t+T_0) + \dot{y}(t-T_0) &= 2\beta_0\dot{y}(t) \end{aligned} \tag{7}$$

The following system of characteristic solutions satisfies system (7):

$$\begin{aligned} y_x(n) &= y(t)\cos vT_0n + [\psi_4(t)\dot{y}(t) \\ &\quad +y(t)(\psi_3(t) - \beta_0)]\frac{\sin vT_0n}{\sin vT_0}, \\ \dot{y}_x(n) &= \dot{y}(t)\cos vT_0n + [\psi_1(t)y(t) \\ &\quad +\dot{y}(t)(\psi_2(t) - \beta_0)]\frac{\sin vT_0n}{\sin vT_0} \end{aligned} \tag{8}$$

Characteristic solutions (8) determine coordinate $y_x(n)$ and velocity $\dot{y}_x(n)$ of an ion over period T_0 starting from $y(t)$ and $\dot{y}(t)$. Other words, characteristic solutions (8) relate to the ion trajectory at moment t.

However, more common systems of equations can be validated by using Eqs. (4) and (6):

$$\begin{aligned} y(t+iT_0) &= \psi_{3,i}y(t) + \psi_{4,i}\dot{y}(t), \\ \dot{y}(t+iT_0) &= \psi_{1,i}y(t) + \psi_{2,i}\dot{y}(t) \end{aligned} \tag{9}$$

and

$$\begin{aligned} y(t-iT_0) &= \psi_{3,-i}y(t) + \psi_{4,-i}\dot{y}(t), \\ \dot{y}(t-iT_0) &= \psi_{1,-i}y(t) + \psi_{2,-i}\dot{y}(t) \end{aligned} \tag{10}$$

and from Eq. (8) we obtain an expression for $\psi_{j,i}$ assuming i instead of n:

$$\psi_{1,i}(t) = \psi_1(t)\frac{\sin vT_0 i}{\sin vT_0},$$
$$\psi_{2,i}(t) = \cos vT_0 i + [\psi_2(t) - \beta_0]\frac{\sin vT_0 i}{\sin vT_0},$$
$$\psi_{3,i}(t) = \cos vT_0 i + [\psi_3(t) - \beta_0]\frac{\sin vT_0 i}{\sin vT_0},$$
$$\psi_{4,i}(t) = \psi_4(t)\frac{\sin vT_0 i}{\sin vT_0} \tag{11}$$

Substituting $-i$ instead of i into Eq. (11), we obtain the respective equations for $\psi_{j,-i}$.

The procedure, developed above, yields an infinite set of characteristic solutions of the Hill equation for different values of i, which can be called an order of a characteristic solution. Such characteristic solutions have the following general form:

$$y_{x,i}(n) = y(t)\cos ivT_0 n + [\psi_{4,i}(t)\dot{y}(t) + y(t)(\psi_{3,i}(t) - \cos ivT_0)]\frac{\sin ivT_0 n}{\sin ivT_0},$$
$$\dot{y}_{x,i}(n) = \dot{y}(t)\cos ivT_0 n + [\psi_{1,i}(t)y(t) + \dot{y}(t)(\psi_{2,i}(t) - \cos ivT_0)]\frac{\sin ivT_0 n}{\sin ivT_0} \tag{12}$$

where

$$\cos vT_0 = \beta_0; \qquad \beta(i) = \cos i(a\cos\beta_0) = \cos ivT_0;$$
$$\sin ivT_0 = (1 - \cos^2 i(a\cos\beta_0))^{1/2}$$

Characteristic solutions (12) determine coordinates and velocities of an ion over period iT_0. In this case, $y(t)$ and $\dot{y}(t)$ are the coordinate and velocity of the ion at the moment when the general solution matches the respective characteristic solution.

Following our methodology, developed in [4], we obtain the following expression for the amplitude of the characteristic solution of order i for the coordinate:

$$Y^2_{m,i} = y^2(t) + \frac{1}{\sin^2 ivT_0} \times [\dot{y}(t)\psi_{4,i}(t) + y(t)\{\psi_{3,i}(t) - \cos ivT_0\}]^2 \tag{13}$$

Now, considering Eqs. (2), (3), (5) and (11), we can show that the following equation is valid for Y^2_m:

$$Y^2_m = -\frac{\psi_{4,1}(t)}{1-\beta_0^2}[\psi_{1,1}(t_0)y_0^2 - y_0\dot{y}_0\{\psi_{3,1}(t_0) - \psi_{2,1}(t_0)\} - \psi_{4,1}(t_0)\dot{y}_0^2] \tag{14}$$

where y_0, $\dot{y}_0$ are the initial coordinate and velocity; t_0 is the initial phase (phase of ion introduction into the rf field); t is the moment when the characteristic solution matches the general solution.

Here we should note that:

- the Eq. (14) obtained here matches completely the analogous equation shown in [4];
- all characteristic solutions have the same values of the extremum amplitude independent of the order i (for the case where t is selected for the maximum $\psi_{4,1}(t)$).

Let us consider Eq. (12). We note that the Y^2_m calculation procedure becomes incorrect when

$$\sin ivT_0 \to 0 \text{ or } \cos i(a\cos\beta_0) \Rightarrow \pm 1 \tag{15}$$

In order to find $y_{x,i}(n)$ and $\dot{y}_{x,i}(n)$ properly for this case, we rewrite Eq. (12) in the following form:

$$y_{x,i}(n) = -y(t)\frac{\sin ivT_0(n-1)}{\sin ivT_0} + y(t + iT_0)\frac{\sin ivT_0 n}{\sin ivT_0},$$
$$\dot{y}_{x,i}(n) = -\dot{y}(t)\frac{\sin ivT_0(n-1)}{\sin ivT_0} + \dot{y}(t + iT_0)\frac{\sin ivT_0 n}{\sin ivT_0} \tag{16}$$

Rearranging Eq. (16) using the Moivre formula and considering Eqs. (15) and (11) we obtain:

$$y_{x,i}(n) = y(t)(\cos ivT_0)^n,$$
$$\dot{y}_{x,i}(n) = \dot{y}(t)(\cos ivT_0)^n \tag{17}$$

It follows from Eq. (17) that if $\cos ivT_0 = +1$ then the general solution of Eq. (1) has the following property: precisely same coordinate and velocity values occur each iT_0 for any integer i. If $\cos ivT_0 = -1$,

then such repetition is observed every $2iT_0$ and, for every iT_0, the coordinate and velocity values show a change of sign only (this has no influence on trapping conditions). This means, for example, that the general solution has a bounded set of various maxima for the case when condition (15) is fulfilled. If the general solution has one maximum during the period T_0 then there could be less than or equal to i different maxima, which repeat in i periods.

Another important conclusion follows from Eq. (17). These expressions are valid for any t and the general solutions, for all points where Eq. (15) is fulfilled, are periodic functions of iT_0 when $\cos ivT_0 = +1$ and they have period of $2iT_0$ when $\cos ivT_0 = -1$. For example, let us consider the working point lying at $\beta_0 = 0$. Then $vT_0 = \pi/2$ and $\cos ivT_0 = \cos i(\pi/2)$. If $i = 2$ then $\cos ivT_0 = -1$. In this case the coordinate and velocity change their signs every $2T_0$, and the general solution has a period of $4T_0$.

Thus, Eq. (15) leads to a different procedure for calculation of the maximum ion excursion from the origin and we should expect that Eq. (14) introduces a considerable error in those points of the stability diagram where Eq. (15) is fulfilled.

We have shown firstly in [6–9] that the stability diagram for QMS has fine structure: the stability diagram contains quasi-stability lines or lines of parametric modulation resonances. It was shown in [7] that these lines degenerate into bands in the presence of nonlinear field distortions within quadrupole mass analyzers. The respective modulation of the rf waveform [8] transforms these lines into instability bands (zones). The equation that determines quasi-stability lines [5,8] matches Eq. (15). Thus, the obtained Eq. (14) is valid

Table 1
The values of stability parameters β_0 for different quasi-stability lines

i	$k = 0$	$k = 1$	$k = 2$	$k = 3$	$k = 4$	$k = 5$
(a) The values of $\beta_{0(-)}$						
1	−1	−1	−1	−1	−1	−1
2	0	0	0	0	0	0
3	0.5	−1	0.5	0.5	−1	0.5
4	0.707107	−0.7071068	−0.707107	0.707107	0.707107	−0.707107
5	0.809017	−0.309017	−1	−0.309017	0.809017	0.809017
6	0.866025	0	−0.866025	−0.866025	0	0.8660254
7	0.900969	0.22252093	−0.62349	−1	−0.62349	0.2225209
8	0.92388	0.38268343	−0.382683	−0.92388	−0.92388	−0.382683
9	0.939693	0.5	−0.173648	−0.766044	−1	−0.766044
10	0.951057	0.58778525	0	−0.587785	−0.95106	−0.951057
	$d = 1$	$d = 2$	$d = 3$	$d = 4$	$d = 5$	$d = 6$
(b) The values of $\beta_{0(+)}$						
1	1	1	1	1	1	1
2	−1	1	−1	1	−1	1
3	−0.5	−0.5	1	−0.5	−0.5	1
4	0	−1	0	1	0	−1
5	0.309017	−0.809017	−0.809017	0.309017	1	0.309017
6	0.5	−0.5	−1	−0.5	0.5	1
7	0.62349	−0.2225209	−0.900969	−0.900969	−0.22252	0.6234898
8	0.707107	0	−0.707107	−1	−0.70711	0
9	0.766044	0.17364818	−0.5	−0.939693	−0.93969	−0.5
10	0.809017	0.30901699	−0.309017	−0.809017	−1	−0.809017
11	0.841254	0.41541501	−0.142315	−0.654861	−0.959493	−0.959493
12	0.866025	0.5	0	−0.5	−0.866025	−1
13	0.885456	0.5680647	0.1205367	−0.354605	−0.748511	−0.970942
14	0.900969	0.6234898	0.2225209	−0.222521	−0.623489	−0.900969

for all points within the stability diagram excluding those points that lie on the quasi-stability lines (or close to them).

It follows from Eq. (12) that parameter $\beta(i)$ is equal to ± 1 on the quasi-stability lines [9]. In this case, the values of β_0 can be calculated as follows:

$$\beta_{0(-)} = \cos\frac{\pi(2k+1)}{i} \quad \text{and} \quad \beta_{0(+)} = \cos\frac{2\pi d}{i},$$

where $k = 0, 1, 2, \ldots$ and $d = 1, 2, 3, \ldots$

The value of $\beta(i) = -1$ corresponds to the $\beta_{0(-)}$ parameter, and $\beta(i) = +1$ corresponds to the $\beta_{0(+)}$ parameter. One can see from the expressions for $\beta_{0(-)}$ and $\beta_{0(+)}$ that there is an infinite set of quasi-stability lines within the stability zone of QMS. The values of $\beta_{0(-)}$ and $\beta_{0(+)}$ calculated for $i = 1, \ldots, 10$, $k = 0, \ldots, 5$ and $d = 1, \ldots, 6$ are shown in Table 1(a) and (b), respectively. These tables are valid for any rf waveform used in QMS. The simplest way to find the extreme values of general solutions of Eq. (1), in the case where the working point of an ion lies on a quasi-stability line, is to use an rf voltage with a rectangular waveform.

3. Calculation of oscillation amplitude for ions, characteristic points of which lie on quasi-stability lines within the stability zone

Fig. 1 illustrates an rf voltage of rectangular waveform. For parameters a_1 and a_2, we have the following

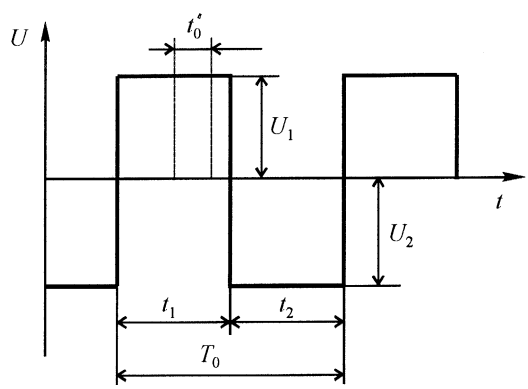

Fig. 1. An rf voltage of rectangular waveform.

expressions:

$$a_1^2 = \frac{2\sigma}{1+n_0+p_0}\frac{U_1 T_0^2}{z_a^2},$$

$$a_2^2 = \frac{2\sigma}{1+n_0+p_0}\frac{U_2 T_0^2}{z_a^2}, \qquad n_0 = \left(\frac{x_a}{z_a}\right)^2,$$

$$p_0 = \left(\frac{x_a}{y_a}\right)^2, \qquad \eta_1 = \frac{t_1}{T_0}, \qquad \eta_2 = \frac{t_2}{T_0}, \tag{18}$$

where σ is the charge-to-mass ratio; x_a, y_a and z_a are the closest distances between the center of the electrode system and the ring and endcap electrodes along the respective axes. For this waveform, the $\psi_{j,1}(t_0')$ functions are calculated as follows [4]:

$$\psi_{1,1}(t_0') = a_1\left\{\cosh a_2\eta_2 \sinh a_1\eta_1 + \frac{1}{2}\left(\frac{a_1}{a_2}+\frac{a_2}{a_1}\right) \times \cosh a_1\eta_1 \sinh a_2\eta_2 + \frac{1}{2}\left(\frac{a_2}{a_1}-\frac{a_1}{a_2}\right) \times \sinh a_2\eta_2 \cosh a_1\eta_1 2t_0'\right\} \tag{19}$$

$$\psi_{2,1}(t_0') = \cosh a_2\eta_2 \cosh a_1\eta_1 + \frac{1}{2}\left(\frac{a_1}{a_2}+\frac{a_2}{a_1}\right) \times \sinh a_2\eta_2 \sinh a_1\eta_1 + \frac{1}{2}\left(\frac{a_1}{a_2}-\frac{a_2}{a_1}\right) \times \sinh a_2\eta_2 \sinh a_1\eta_1 2t_0' \tag{20}$$

$$\psi_{3,1}(t_0') = \cosh a_2\eta_2 \cosh a_1\eta_1 + \frac{1}{2}\left(\frac{a_1}{a_2}+\frac{a_2}{a_1}\right) \times \sinh a_2\eta_2 \sinh a_1\eta_1 + \frac{1}{2}\left(\frac{a_2}{a_1}-\frac{a_1}{a_2}\right) \times \sinh a_2\eta_2 \sinh a_1\eta_1 2t_0' \tag{21}$$

$$\psi_{4,1}(t_0') = \frac{1}{a_1}\left\{\cosh a_2\eta_2 \sinh a_1\eta_1 + \frac{1}{2}\left(\frac{a_1}{a_2}+\frac{a_2}{a_1}\right) \times \cosh a_1\eta_1 \sinh a_2\eta_2 + \frac{1}{2}\left(\frac{a_1}{a_2}-\frac{a_2}{a_1}\right) \times \sinh a_2\eta_2 \cosh a_1\eta_1 2t_0'\right\} \tag{22}$$

Let us consider ion injection during the focusing pulse at the phase t_0'. In this case we can find the

coordinate $\bar{y}_0$ and velocity $\dot{\bar{y}}_0$ at the beginning of the focusing pulse by using the initial parameters of ion motion. For this purpose simple equations can be used:

$$\bar{y}_0 = y_0 \cos a_1\eta_1\left(\frac{1}{2}+t_0'\right) - \frac{\dot{y}_0}{a_1}\sin a_1\eta_1\left(\frac{1}{2}+t_0'\right) \tag{23}$$

$$\dot{\bar{y}}_0 = a_1\left[y_0 \sin a_1\eta_1\left(\frac{1}{2}+t_0'\right) + \frac{\dot{y}_0}{a_1}\cos a_1\eta_1\left(\frac{1}{2}+t_0'\right)\right] \tag{24}$$

Now, using Eq. (8), we find the coordinate and velocity of the ion at the beginning of the nth period of the rf field and its extreme displacement from the origin of the coordinates for an arbitrary period:

$$Y_{\mathrm{m_f}}^2(n) = y_x^2(n) + \frac{1}{a_1^2}\dot{y}_x^2(n) \tag{25}$$

where index f indicates the focusing pulse; $y_x(n)$ and $\dot{y}_x(n)$ are given by:

$$y_x(n) = \bar{y}_0 \cos \upsilon T_0 n + [\bar{\psi}_{4,1}\dot{\bar{y}}_0 + \bar{y}_0(\bar{\psi}_{3,1} - \beta_0)] \times \frac{\sin \upsilon T_0 n}{\sin \upsilon T_0} \tag{26}$$

$$\dot{y}_x(n) = \dot{\bar{y}}_0 \cos \upsilon T_0 n + [\bar{\psi}_{1,1}\bar{y}_0 + \dot{\bar{y}}_0(\bar{\psi}_{2,1} - \beta_0)] \times \frac{\sin \upsilon T_0 n}{\sin \upsilon T_0} \tag{27}$$

The values of $\bar{\psi}_{j,1}$ can be found using Eqs. (19)–(22). Here we assume that $t_0' = -0.5$; a_1 is an imaginary quantity and a_2 is a real quantity.

Using Eq. (25), we calculate the first extremum for $n = 0$, the second extremum for $n = 1$, etc. If the ion is injected during the defocusing pulse then the initial parameters are transformed as follows:

$$\bar{y}_0 = y_0 \cosh a_2\eta_2\left(\frac{1}{2}-t_0'\right) + \frac{\dot{y}_0}{a_2}\sinh a_2\eta_2\left(\frac{1}{2}-t_0'\right),$$

$$\dot{\bar{y}}_0 = a_2\left[y_0 \sinh a_2\eta_2\left(\frac{1}{2}-t_0'\right) + \frac{\dot{y}_0}{a_2}\cosh a_2\eta_2\left(\frac{1}{2}-t_0'\right)\right] \tag{28}$$

Substituting Eq. (28) into Eqs. (26) and (27), we obtain extrema for different n.

Let us consider an example of how the amplitude of ion oscillation can be calculated for the case where the working point lies on the quasi-stability line $\beta_0 = 0$. We assume here that the field within the QMS is created by bipolar pulses with equal amplitudes (EA mode). This is a very promising rf voltage and its particular case is a 50% duty-cycle symmetric rectangular waveform or "meander."

In this case, $i = 2$, as follows from Eq. (15). This means that there are only two different extrema (or only one) for the general solution of Eq. (1). The values of these extrema for $n = 0$ (the first extremum) and for $n = 1$ (the second extremum) are calculated using Eqs. (25)–(27). In this case, the expressions for $\bar{\psi}_{1,1}$ can be simplified:

$$\bar{\psi}_{1,1} = -a_1 \cosh a_1\eta_2, \qquad \bar{\psi}_{2,1} = \sinh a_1\eta_2,$$
$$\bar{\psi}_{3,1} = -\sinh a_1\eta_2, \qquad \bar{\psi}_{4,1} = \frac{1}{a_1}\cosh a_1\eta_2,$$
$$a_1 = \frac{\pi}{2\eta_1} \tag{29}$$

Now, using Eqs. (25)–(27), we obtain:

$$Y_{\mathrm{m_f}}^2(0) = y_0^2 + \frac{\dot{y}_0^2}{a_1^2} \tag{30}$$

$$Y_{\mathrm{m_f}}^2(1) = y_0^2\left[\cosh 2a_1\eta_2 - \sinh 2a_1\eta_2 \cos 2a_1\eta_1 t_0'\right] + 2y_0\frac{\dot{y}_0}{a_1}\sinh 2a_1\eta_2 \sin 2a_1\eta_1 t_0' + \frac{\dot{y}_0^2}{a_1^2} \times \left[\cosh 2a_1\eta_2 + \sinh 2a_1\eta_2 \cos 2a_1\eta_1 t_0'\right] \tag{31}$$

$$Y_{\mathrm{m_{df}}}^2(0) = y_0^2 \cosh a_1\eta_2(1-2t_0') + 2y_0\frac{\dot{y}_0}{a_1}\sinh a_1\eta_2 \times(1-2t_0') + \frac{\dot{y}_0^2}{a_1^2}\cosh a_1\eta_2(1-2t_0') \tag{32}$$

$$Y_{\mathrm{m_{df}}}^2(1) = y_0^2 \cosh a_1\eta_2(1+2t_0') - 2y_0\frac{\dot{y}_0}{a_1}\sinh a_1\eta_2 \times(1+2t_0') + \frac{\dot{y}_0^2}{a_1^2}\cosh a_1\eta_2(1+2t_0') \tag{33}$$

where f and df represent the focusing and defocusing pulses, respectively.

It follows from Eqs. (30) and (31) that the maximum ion excursion from the origin does not depend on the initial phase t'_0 if $Y^2_{m_f}(0) > Y^2_{m_f}(1)$. It can be shown that the minimal value of $Y^2_{m_f}(1)$ is given by:

$$Y^2_{m_f}(1)_{(min)} = \left(y_0^2 + \frac{\dot{y}_0^2}{\pi^2}\right)\exp(-\pi) \tag{34}$$

for phase t'_{00}

$$\mathrm{tg}\, 2a_1\eta_1 t'_{00} = -\frac{2y_0(\dot{y}_0/\pi)}{y_0^2 - (\dot{y}_0^2/\pi)} \tag{35}$$

For a working point lying on the $\beta_0 = 0$ quasi-stability line, there is a range of phases within the focusing pulse with a constant oscillation amplitude. This phase range lies in the neighborhood of phase t'_{00} given by Eq. (35). It follows from Eq. (31) that $Y^2_{m_f}(1)$ increases at phases t'_0 lying at the edges of the focusing pulse ($t'_0 = \pm 0.5$) up to the value:

$$Y^2_{m_f}(1) = \left[y_0^2 + \frac{\dot{y}_0^2}{a_1^2}\right]\cosh 2a_1\eta_2 + 2y_0\frac{\dot{y}_0}{a_1}\sinh 2a_1\eta_2 \tag{36}$$

and becomes greater than $Y^2_{m_f}(0)$. At phase t'_0 that corresponds to the optimal phase of the first kind ($t'_0 = 0$) the following equation can be obtained from Eq. (31):

$$Y^2_{m_f}(1)|_{t'_0=0} = y_0^2\exp(-2a_1\eta_2) + \frac{\dot{y}_0^2}{a_1^2}\exp(2a_1\eta_2) \tag{37}$$

Comparing this equation with Eq. (30), we notice that $Y^2_{m_f}(0) > Y^2_{m_f}(1)$ for low values of $\dot{y}_0$ and the "plateau" at the maximum amplitude vs. the injection phase curve includes the optimal phase of the first kind. The optimal phase of the first kind does not lie at the "plateau" if the initial velocity exceeds the critical velocity $\dot{y}_{0\,cr} = 0.6531\dot{y}_0$; the "plateau" narrows but still lies around phase t'_{00} (see Eq. (35)).

If an ion is injected at a phase of the focusing pulse then the maximum ion excursion changes with t'_0 according to Eqs. (32) and (33).

Now we compare calculations of maximum ion excursion from the origin using Eq. (14) and Eqs. (30)–(33) for the working points lying at the $\beta_0 = 0$ quasi-stability line (for $\eta_1 = \eta_2$).

For the optimal phase of the first kind we have:

$$\left.\frac{Y^2_{m\,Eq.\,(14)}}{Y^2_{m\,Eq.\,(30)}}\right|_{\beta_0=0} = 1.24377 \tag{38}$$

Thus, the general expression (14) yields an error of 24.4% for the amplitude of ion excursion at the points lying at the $\beta_0 = 0$ quasi-stability line. This calculation was made for $y_0 = 1$, $\dot{y}_0 = -0.5$ and $U_{p-p} = 10^3$ V that corresponds to an injection energy of 4.22 eV (the type of waveform is here the "meander" with zero dc component, $\eta_1 = \eta_2$).

If the injection phase moves from the optimal phase of the first kind towards the edge of the focusing pulse, then the value of the ratio given by Eq. (38) changes and its value decreases to 1.078. This means that the calculation error of Eq. (14) decreases to about 8%.

If the ion is injected at phases of the defocusing pulse then one should use Eqs. (32) and (33). For the case where the initial phase coincides with the optimal phase of the second kind ($t'_0 = 0$), Eq. (33) yields a greater value of Y^2_m than the value calculated using Eq. (32) and the initial conditions described above (negative injection energy). Here we use Eq. (33).

For this case, we make the following estimation:

$$\left.\frac{Y^2_{m\,Eq.\,(14)}}{Y^2_{m\,Eq.\,(33)}}\right|_{\beta_0=0} = 1.49226 \tag{39}$$

Here we obtain a greater deviation (about 50%) in comparison with the case considered above.

In practice, to evaluate ion trap performance, so called amplitude-phase characteristics (APC) of the first and second kinds are used. The APC of the first kind is the dependence of the amplitude of the oscillatory ion motion on the injection phase calculated for the following initial conditions: $y_0 = 1$, $\dot{y}_0 = 0$. The APC of the second kind is calculated for $y_0 = 0$, $\dot{y}_0 = 1$.

The APC of the first kind, as follows from Eq. (14), is described by the following expression:

$$Y^2_m|_{(1,0)} = -\frac{\psi_{4,1}(t)\psi_{1,1}(t'_0)}{1-\beta_0^2} \tag{40}$$

The theory developed above allows us to obtain the APC of the first and second kinds for the case where the working point lies on a quasi-stability line. For this purpose, for example for $\beta_0 = 0$, we can use Eqs. (30) and (31) if the initial phase corresponds to the focusing pulse, and Eqs. (32) and (33) if the initial phase lies within the defocusing pulse. Thus, Eqs. (30) and (31) for the focusing pulse yield two expressions to describe the APC of the first kind:

$$Y^2_{m_{1_f}}|_{(1,0)} = [\cosh\pi - \sinh\pi\cos\pi t'_0] \tag{41}$$

and

$$Y^2_{m_{1_f}}|_{(1,0)} = 1 \tag{42}$$

We see that the oscillation amplitude calculated from Eq. (41) for the optimal phase of the first kind ($t'_0 = 0$) is less than the amplitude obtained from Eq. (42). Thus, in the neighborhood of this phase, one should use Eq. (42) up to the critical phase $t'_{0\,cr}$ that corresponds to the following condition:

$$\cosh\pi - \sinh\pi\cos\pi t'_{0\,cr} = 1 \tag{43}$$

or

$$t'_{0\,cr} = 0.1305$$

For phases $t'_0 > t'_{0\,cr}$ lying within the focusing pulse, the APC of the first kind is derived using Eq. (41). At the edges of the focusing pulse we have:

$$Y^2_{m_{1_f}}(1,0) = \cosh\pi = 11.592$$

The APC of the first kind determined by Eq. (40) has the value of $Y^2_m|_{(1,0)}$ equal to 1 at the optimal phase of the first kind (Eq. (42) yields the same value) and at the edges of the focusing pulse:

$$Y^2_m|_{(1,0)} = 12.07$$

Thus, the APC of the first kind calculated using Eq. (14) has one minimum equal to 1. The other values of amplitudes are greater than those of amplitudes calculated from Eqs. (41) and (42). However, the remarkable property of the APC obtained from Eqs. (41) and (42) is that this curve has a "plateau" about the minimum.

The APC of the first kind for the phases within the defocusing pulse, as follows from Eq. (14), is described by:

$$Y^2_{m_{df}}|_{(1,0)} = \exp\left(\frac{\pi}{2}\right)\cosh\pi t'_0 \tag{44}$$

The value of $Y^2_{m_{df}}(1,0)$ at the optimal phase of the second kind ($t'_0 = 0$) is equal to 4.81, and at the edges of the defocusing pulse:

$$Y^2_{m_{df}}|_{(1,0)} = \exp\left(\frac{\pi}{2}\right)\cosh\frac{\pi}{2} = 12.07 \tag{45}$$

Now, we obtain an expression for the APC of the first kind within the defocusing pulse for $\beta_0 = 0$.

From Eqs. (32) and (33) we have:

$$Y^2_{m_{df}}(0)|_{(1,0)} = \cosh a_1\eta_1(1 - 2t'_0) \quad \text{and}$$
$$Y^2_{m_{df}}(1)|_{(1,0)} = \cosh a_1\eta_1(1 + 2t'_0) \tag{46}$$

It follows from Eq. (46) that the values of $Y^2_{m_{df}}(0)|_{(1,0)}$ and $Y^2_{m_{df}}(1)|_{(1,0)}$ are equal to each other at the optimal phase of the second kind ($t'_0 = 0$) and differ at the edges of the pulse ($t'_0 = \pm 0.5$). This means that the APC of the first kind has a minimum at $t'_0 = 0$:

$$Y^2_{m_{df}}|_{\substack{(1,0)\\(t'_0=0)}} = \cosh\frac{\pi}{2} = 2.51 \tag{47}$$

At the edges of the defocusing pulse ($t'_0 = \pm 0.5$):

$$Y^2_{m_{df}}|_{\substack{(1,0)\\(t'_0=\pm 0.5)}} = \cosh\pi = 11.59 \tag{48}$$

Comparing Eqs. (47) and (48) with Eqs. (44) and (45) (obtained from Eq. (14)), we see that Eq. (14) yields a minimum value twice as large as that obtained from Eq. (47); the APC of the first kind, calculated using Eq. (14), exhibits greater values by 4% at the edges of the defocusing pulse. Thus, the APC of the first kind goes above the true curve within the defocusing pulse.

APC of the first and second kinds are used to estimate the trapping efficiency for different ion injection techniques. If the ionizing electron beam is injected through a narrow slit in the ring electrode then the ions created have small initial velocities in the *XY* plane, but considerable initial coordinates. In this case, the trapping efficiency in the *XY* plane is determined by

the APC of the first kind for the $x(y)$ coordinate; the trapping efficiency for ions along the Z axis is determined by the APC of the second kind. Alternatively, if a narrow ionizing electron beam is injected along the Z axis, then the trapping efficiency in the XY plane is determined by the APC of the second kind for the $x(y)$ coordinate, and the APC of the first kind for the z coordinate is important for the trapping efficiency along the Z axis.

From Eq. (14) we obtain the APC of the second kind in the following form:

$$Y^2_{\mathrm{m}}|_{(0,1)} = \frac{\psi_{4,1}(t)\psi_{4,1}(t_0)}{1-\beta_0^2} \tag{49}$$

If $\beta_0 = 0$, then for a rectangular rf waveform (meander, $\eta_1 = \eta_2$ with zero dc component) we have:

$$Y^2_{\mathrm{m_f}}(0)|_{(0,1)} = \frac{1}{a_1^2} \tag{50}$$

$$Y^2_{\mathrm{m_f}}(1)|_{(0,1)} = \frac{1}{a_1^2}(\cosh\pi + \sinh\pi\cos\pi t_0') \tag{51}$$

and

$$Y^2_{\mathrm{m_{df}}}(0)|_{(0,1)} = \frac{1}{a_1^2}\cosh\frac{\pi}{2}(1-2t_0') \tag{52}$$

$$Y^2_{\mathrm{m_{df}}}(1)|_{(0,1)} = \frac{1}{a_1^2}\cosh\frac{\pi}{2}(1+2t_0') \tag{53}$$

It follows from Eqs. (50) and (51) that the shape of the APC of the second kind is determined by Eq. (51) only and there is one maximum in the middle of the focusing pulse at $t_0' = 0$. The value of the maximum is:

$$Y^2_{\mathrm{m_{f_{max}}}}|_{(0,1)} = \frac{1}{\pi^2}\exp(\pi) = 2.34 \tag{54}$$

At the edges of the focusing pulse, the APC possesses the following value:

$$Y^2_{\mathrm{m_{f_{min}}}}|_{(0,1)} = \frac{1}{\pi^2}\cosh\pi = 1.174 \tag{55}$$

The APC of the second kind, as follows from Eqs. (52) and (53), has a minimum in the middle of the defocusing pulse:

$$Y^2_{\mathrm{m_{df_{min}}}}|_{(0,1)} = \frac{1}{\pi^2}\cosh\frac{\pi}{2} = 0.2542 \tag{56}$$

and two maxima at the edges of the defocusing pulse whose values coincide with those obtained from Eq. (55).

Eq. (49) yields the value of 2.34 (that matches Eq. (54)) for the APC of the second kind in the middle of the focusing pulse, and

$$Y^2_{\mathrm{m_f\ Eq.\ (49)}}|_{(0,1)} = \frac{1}{\pi^2}\exp\left(\frac{\pi}{2}\right)\cosh\frac{\pi}{2} = 1.223 \tag{57}$$

at the edges; this value is 4% greater than that obtained from Eq. (55).

For the defocusing pulse, we obtain from Eq. (49):

$$Y^2_{\mathrm{m_{df}\ Eq.\ (49)}}|_{(0,1)} = \frac{1}{\pi^2}\exp\left(\frac{\pi}{2}\right)\cosh\pi t_0' \tag{58}$$

Here, the minimum is in the middle of the pulse, and its value is 0.487. This is almost twice as large as the value obtained from Eq. (50). Eq. (58) yields a maximum value at $t_0' = \pm 0.5$ that matches the value determined from Eq. (57), but is greater than the value of Eq. (55).

Thus, Eq. (14) gives an inflated APC of the both kinds within the whole period T_0.

At the end of this part, the author is ready to answer a reader's basic question: what is a real reason for the disagreement between the amplitudes of ion oscillations determined from different expressions? Now we can say surely: the main reason of this disagreement is that the oscillation amplitude vs. the parameter stability curve has a spiking structure. This means that the amplitude of ion oscillatory motion decreases sharply if the working point on the stability diagram approaches a quasi-stability line (parametric resonance line). Thus, the revealed spiking structure of the dependence between the oscillation amplitude and the working point location is determined completely by the fine structure of the stability diagram, about which we have reported previously [6,9,10].

In Part II of this article, we investigate the fine effects discovered in the amplitude of ion oscillations within the QMS and we compare the values of amplitudes calculated from the obtained analytical expressions and by direct trajectory calculations.

4. Conclusions

The general theory of characteristic solution method is demonstrated and the fundamental expressions determining the amplitude of ion oscillation within the QMS are presented here. It is shown that there is a spiking structure in the dependence between the amplitude of ion oscillation and the working point location on the stability diagram. This spiking structure occurs due to the fine structure of the stability diagram the existence of which has been pointed out in our earlier works.

References

[1] E.P. Sheretov, B.I. Kolotilin, J. Tech. Phys. XII (9) (1972) 1931.
[2] E.P. Sheretov, Terent'ev, J. Tech. Phys. XII (5) (1972) 953.
[3] E.P. Sheretov, Int. J. Mass Spectrom. 198 (2000) 83.
[4] E.P. Sheretov, B.I. Kolotilin, N.V. Veselkin, A.V. Brykov, E.V. Fedosov, Int. J. Mass Spectrom. 198 (2000) 97.
[5] N.W. McLachlan, Theory and Applications of Mathieu Functions, Clarendon, Oxford, 1947.
[6] E.P. Sheretov, B.I. Kolotilin, A structure of the stability diagram for quadrupole mass spectrometers (in Russian), Scientific Digest (Nauchnoe priborostroenie), Ryazan State Radio Technical University, Ryazan, 1995, p. 3.
[7] E.P. Sheretov, B.I. Kolotilin, O.W. Rozhkov, Modulation resonances in hyperboloidal mass spectrometers (in Russian), Scientific Digest (Nauchnoe priborostroenie), Ryazan State Radio Technical University, Ryazan, 1995, p. 8.
[8] E.P. Sheretov, B.I. Kolotilin, M.P. Safonov, Nonlinear resonances in hyperboloidal mass spectrometry (in Russian), Scientific Digest (Nauchnoe priborostroenie), Ryazan State Radio Technical University, Ryazan, 1995, p. 18.
[9] E.P. Sheretov, V.S. Gurov, B.I. Kolotilin, Int. J. Mass Spectrom. 184 (1999) 207.
[10] E.P. Sheretov, B.I. Kolotilin, A.V. Brykov, A.E. Sheretov, in: Proceedings of the 14th International Mass Spectrometry Conference, Tampere, Finland, August, 1997, p. 229.